



**Fermi National Accelerator Laboratory**

**FERMILAB-Conf-95/214-E**

**D0**

**Studies of Topological Distributions of the Three- and Four-Jet Events in  $\bar{p}p$  Collisions at  $\sqrt{s} = 1800$  GeV with the D0 Detector**

S. Abachi et al.

The D0 Collaboration

*Fermi National Accelerator Laboratory  
P.O. Box 500, Batavia, Illinois 60510*

July 1995

Submitted to the *International Europhysics Conference on High Energy Physics (HEP95)*,  
Brussels, Belgium, July 27-August 2, 1995

## Disclaimer

*This report was prepared as an account of work sponsored by an agency of the United States Government. Neither the United States Government nor any agency thereof, nor any of their employees, makes any warranty, expressed or implied, or assumes any legal liability or responsibility for the accuracy, completeness, or usefulness of any information, apparatus, product, or process disclosed, or represents that its use would not infringe privately owned rights. Reference herein to any specific commercial product, process, or service by trade name, trademark, manufacturer, or otherwise, does not necessarily constitute or imply its endorsement, recommendation, or favoring by the United States Government or any agency thereof. The views and opinions of authors expressed herein do not necessarily state or reflect those of the United States Government or any agency thereof.*

# Studies of Topological Distributions of the Three- and Four-Jet Events in $\bar{p}p$ Collisions at $\sqrt{s} = 1800$ GeV with the DØ Detector

The DØ Collaboration<sup>1</sup>  
(July 1995)

---

The global topologies of three- and four-jet events produced in  $\bar{p}p$  interactions are described. The three- and four-jet events are selected from data recorded by the DØ detector at the Tevatron Collider operating at a center-of-mass energy of  $\sqrt{s} = 1800$  GeV. The measured normalized distributions of various topological variables are compared with parton-level predictions of the tree-level QCD calculations. The parton-level QCD calculations are found to be in good agreement with the data. The studies also show that the topological distributions of the different subprocesses involving different numbers of quarks are very similar and reproduce the measured distributions well.

---

S. Abachi,<sup>12</sup> B. Abbott,<sup>34</sup> M. Abolins,<sup>23</sup> B.S. Acharya,<sup>41</sup> I. Adam,<sup>10</sup> D.L. Adams,<sup>35</sup> M. Adams,<sup>15</sup>  
S. Ahn,<sup>12</sup> H. Aihara,<sup>20</sup> J. Alitti,<sup>37</sup> G. Álvarez,<sup>16</sup> G.A. Alves,<sup>8</sup> E. Amidi,<sup>27</sup> N. Amos,<sup>22</sup>  
E.W. Anderson,<sup>17</sup> S.H. Aronson,<sup>3</sup> R. Astur,<sup>39</sup> R.E. Avery,<sup>29</sup> A. Baden,<sup>21</sup> V. Balamurali,<sup>30</sup>  
J. Balderston,<sup>14</sup> B. Baldin,<sup>12</sup> J. Bantly,<sup>4</sup> J.F. Bartlett,<sup>12</sup> K. Bazizi,<sup>7</sup> J. Bendich,<sup>20</sup> S.B. Beri,<sup>32</sup>  
I. Bertram,<sup>35</sup> V.A. Bezzubov,<sup>33</sup> P.C. Bhat,<sup>12</sup> V. Bhatnagar,<sup>32</sup> M. Bhattacharjee,<sup>11</sup> A. Bischoff,<sup>7</sup>  
N. Biswas,<sup>30</sup> G. Blazey,<sup>12</sup> S. Blessing,<sup>13</sup> P. Bloom,<sup>5</sup> A. Boehnlein,<sup>12</sup> N.I. Bojko,<sup>33</sup>  
F. Borcherding,<sup>12</sup> J. Borders,<sup>36</sup> C. Boswell,<sup>7</sup> A. Brandt,<sup>12</sup> R. Brock,<sup>23</sup> A. Bross,<sup>12</sup> D. Buchholz,<sup>29</sup>  
V.S. Burtovoi,<sup>33</sup> J.M. Butler,<sup>12</sup> D. Casey,<sup>36</sup> H. Castilla-Valdez,<sup>9</sup> D. Chakraborty,<sup>39</sup>  
S.-M. Chang,<sup>27</sup> S.V. Chekulaev,<sup>33</sup> L.-P. Chen,<sup>20</sup> W. Chen,<sup>39</sup> L. Chevalier,<sup>37</sup> S. Chopra,<sup>32</sup>  
B.C. Choudhary,<sup>7</sup> J.H. Christenson,<sup>12</sup> M. Chung,<sup>15</sup> D. Claes,<sup>39</sup> A.R. Clark,<sup>20</sup> W.G. Cobau,<sup>21</sup>  
J. Cochran,<sup>7</sup> W.E. Cooper,<sup>12</sup> C. Cretsinger,<sup>36</sup> D. Cullen-Vidal,<sup>4</sup> M.A.C. Cummings,<sup>14</sup> D. Cutts,<sup>4</sup>  
O.I. Dahl,<sup>20</sup> K. De,<sup>42</sup> M. Demarteau,<sup>12</sup> R. Demina,<sup>27</sup> K. Denisenko,<sup>12</sup> N. Denisenko,<sup>12</sup>  
D. Denisov,<sup>12</sup> S.P. Denisov,<sup>33</sup> W. Dharmaratna,<sup>13</sup> H.T. Diehl,<sup>12</sup> M. Diesburg,<sup>12</sup> G. Di Loreto,<sup>23</sup>  
R. Dixon,<sup>12</sup> P. Draper,<sup>42</sup> J. Drinkard,<sup>6</sup> Y. Ducros,<sup>37</sup> S.R. Dugad,<sup>41</sup> S. Durston-Johnson,<sup>36</sup>  
D. Edmunds,<sup>23</sup> J. Ellison,<sup>7</sup> V.D. Elvira,<sup>12,‡</sup> R. Engelmann,<sup>39</sup> S. Eno,<sup>21</sup> G. Eppley,<sup>35</sup>  
P. Ermolov,<sup>24</sup> O.V. Eroshin,<sup>33</sup> V.N. Evdokimov,<sup>33</sup> S. Fahey,<sup>23</sup> T. Fahland,<sup>4</sup> M. Fatyga,<sup>3</sup>  
M.K. Fatyga,<sup>36</sup> J. Featherly,<sup>3</sup> S. Feher,<sup>39</sup> D. Fein,<sup>2</sup> T. Ferbel,<sup>36</sup> G. Finocchiaro,<sup>39</sup> H.E. Fisk,<sup>12</sup>  
Yu. Fisyak,<sup>24</sup> E. Flattum,<sup>23</sup> G.E. Forden,<sup>2</sup> M. Fortner,<sup>28</sup> K.C. Frame,<sup>23</sup> P. Franzini,<sup>10</sup> S. Fuess,<sup>12</sup>  
A.N. Galjaev,<sup>33</sup> E. Gallas,<sup>42</sup> C.S. Gao,<sup>12,\*</sup> S. Gao,<sup>12,\*</sup> T.L. Geld,<sup>23</sup> R.J. Genik II,<sup>23</sup> K. Genser,<sup>12</sup>  
C.E. Gerber,<sup>12,§</sup> B. Gibbard,<sup>3</sup> V. Glebov,<sup>36</sup> S. Glenn,<sup>5</sup> B. Gobbi,<sup>29</sup> M. Goforth,<sup>13</sup>  
A. Goldschmidt,<sup>20</sup> B. Gómez,<sup>1</sup> P.I. Goncharov,<sup>33</sup> H. Gordon,<sup>3</sup> L.T. Goss,<sup>43</sup> N. Graf,<sup>3</sup>  
P.D. Grannis,<sup>39</sup> D.R. Green,<sup>12</sup> J. Green,<sup>28</sup> H. Greenlee,<sup>12</sup> G. Griffin,<sup>6</sup> N. Grossman,<sup>12</sup>  
P. Grudberg,<sup>20</sup> S. Grünendahl,<sup>36</sup> W. Gu,<sup>12,\*</sup> G. Guglielmo,<sup>31</sup> J.A. Guida,<sup>39</sup> J.M. Guida,<sup>3</sup>  
W. Guryn,<sup>3</sup> S.N. Gurzhiev,<sup>33</sup> P. Gutierrez,<sup>31</sup> Y.E. Gutnikov,<sup>33</sup> N.J. Hadley,<sup>21</sup> H. Haggerty,<sup>12</sup>  
S. Hagopian,<sup>13</sup> V. Hagopian,<sup>13</sup> K.S. Hahn,<sup>36</sup> R.E. Hall,<sup>6</sup> S. Hansen,<sup>12</sup> R. Hatcher,<sup>23</sup>  
J.M. Hauptman,<sup>17</sup> D. Hedin,<sup>28</sup> A.P. Heinson,<sup>7</sup> U. Heintz,<sup>12</sup> R. Hernández-Montoya,<sup>9</sup>  
T. Heuring,<sup>13</sup> R. Hirosky,<sup>13</sup> J.D. Hobbs,<sup>12</sup> B. Hoeneisen,<sup>1,¶</sup> J.S. Hoftun,<sup>4</sup> F. Hsieh,<sup>22</sup> Ting Hu,<sup>39</sup>

---

<sup>1</sup>Submitted to the XVII International Symposium on Lepton-Photon Interactions (LP95), Beijing, China, August 10-15, 1995.

Tong Hu,<sup>16</sup> T. Huehn,<sup>7</sup> S. Igarashi,<sup>12</sup> A.S. Ito,<sup>12</sup> E. James,<sup>2</sup> J. Jaques,<sup>30</sup> S.A. Jerger,<sup>23</sup>  
 J.Z.-Y. Jiang,<sup>39</sup> T. Joffe-Minor,<sup>29</sup> H. Johari,<sup>27</sup> K. Johns,<sup>2</sup> M. Johnson,<sup>12</sup> H. Johnstad,<sup>40</sup>  
 A. Jonckheere,<sup>12</sup> M. Jones,<sup>14</sup> H. Jöstlein,<sup>12</sup> S.Y. Jun,<sup>29</sup> C.K. Jung,<sup>39</sup> S. Kahn,<sup>3</sup> G. Kalbfleisch,<sup>31</sup>  
 J.S. Kang,<sup>18</sup> R. Kehoe,<sup>30</sup> M.L. Kelly,<sup>30</sup> A. Kernan,<sup>7</sup> L. Kerth,<sup>20</sup> C.L. Kim,<sup>18</sup> S.K. Kim,<sup>38</sup>  
 A. Klatchko,<sup>13</sup> B. Klima,<sup>12</sup> B.I. Klochkov,<sup>33</sup> C. Klopfenstein,<sup>39</sup> V.I. Klyukhin,<sup>33</sup>  
 V.I. Kochetkov,<sup>33</sup> J.M. Kohli,<sup>32</sup> D. Koltick,<sup>34</sup> A.V. Kostritskiy,<sup>33</sup> J. Kotcher,<sup>3</sup> J. Kourlas,<sup>26</sup>  
 A.V. Kozelov,<sup>33</sup> E.A. Kozlovski,<sup>33</sup> M.R. Krishnaswamy,<sup>41</sup> S. Krzywdzinski,<sup>12</sup> S. Kunori,<sup>21</sup>  
 S. Lami,<sup>39</sup> G. Landsberg,<sup>12</sup> R.E. Lanou,<sup>4</sup> J-F. Lebrat,<sup>37</sup> A. Leflat,<sup>24</sup> H. Li,<sup>39</sup> J. Li,<sup>42</sup> Y.K. Li,<sup>29</sup>  
 Q.Z. Li-Demarteau,<sup>12</sup> J.G.R. Lima,<sup>8</sup> D. Lincoln,<sup>22</sup> S.L. Linn,<sup>13</sup> J. Linnemann,<sup>23</sup> R. Lipton,<sup>12</sup>  
 Y.C. Liu,<sup>29</sup> F. Lobkowicz,<sup>36</sup> S.C. Loken,<sup>20</sup> S. Lökös,<sup>39</sup> L. Lueking,<sup>12</sup> A.L. Lyon,<sup>21</sup>  
 A.K.A. Maciel,<sup>8</sup> R.J. Madaras,<sup>20</sup> R. Madden,<sup>13</sup> I.V. Mandrichenko,<sup>33</sup> Ph. Mangeot,<sup>37</sup> S. Mani,<sup>5</sup>  
 B. Mansoulié,<sup>37</sup> H.S. Mao,<sup>12,\*</sup> S. Margulies,<sup>15</sup> R. Markeloff,<sup>28</sup> L. Markosky,<sup>2</sup> T. Marshall,<sup>16</sup>  
 M.I. Martin,<sup>12</sup> M. Marx,<sup>39</sup> B. May,<sup>29</sup> A.A. Mayorov,<sup>33</sup> R. McCarthy,<sup>39</sup> T. McKibben,<sup>15</sup>  
 J. McKinley,<sup>23</sup> T. McMahon,<sup>31</sup> H.L. Melanson,<sup>12</sup> J.R.T. de Mello Neto,<sup>8</sup> K.W. Merritt,<sup>12</sup>  
 H. Miettinen,<sup>35</sup> A. Milder,<sup>2</sup> A. Mincer,<sup>26</sup> J.M. de Miranda,<sup>8</sup> C.S. Mishra,<sup>12</sup>  
 M. Mohammadi-Baarmand,<sup>39</sup> N. Mokhov,<sup>12</sup> N.K. Mondal,<sup>41</sup> H.E. Montgomery,<sup>12</sup> P. Mooney,<sup>1</sup>  
 M. Mudan,<sup>26</sup> C. Murphy,<sup>16</sup> C.T. Murphy,<sup>12</sup> F. Nang,<sup>4</sup> M. Narain,<sup>12</sup> V.S. Narasimham,<sup>41</sup>  
 A. Narayanan,<sup>2</sup> H.A. Neal,<sup>22</sup> J.P. Negret,<sup>1</sup> E. Neis,<sup>22</sup> P. Nemethy,<sup>26</sup> D. Nešić,<sup>4</sup> D. Norman,<sup>43</sup>  
 L. Oesch,<sup>22</sup> V. Oguri,<sup>8</sup> E. Oltman,<sup>20</sup> N. Oshima,<sup>12</sup> D. Owen,<sup>23</sup> P. Padley,<sup>35</sup> M. Pang,<sup>17</sup> A. Para,<sup>12</sup>  
 C.H. Park,<sup>12</sup> Y.M. Park,<sup>19</sup> R. Partridge,<sup>4</sup> N. Parua,<sup>41</sup> M. Paterno,<sup>36</sup> J. Perkins,<sup>42</sup> A. Peryshkin,<sup>12</sup>  
 M. Peters,<sup>14</sup> H. Piekarz,<sup>13</sup> Y. Pischalnikov,<sup>34</sup> A. Pluquet,<sup>37</sup> V.M. Podstavkov,<sup>33</sup> B.G. Pope,<sup>23</sup>  
 H.B. Prosper,<sup>13</sup> S. Protopopescu,<sup>3</sup> D. Pušeljčić,<sup>20</sup> J. Qian,<sup>22</sup> P.Z. Quintas,<sup>12</sup> R. Raja,<sup>12</sup>  
 S. Rajagopalan,<sup>39</sup> O. Ramirez,<sup>15</sup> M.V.S. Rao,<sup>41</sup> P.A. Rapidis,<sup>12</sup> L. Rasmussen,<sup>39</sup> A.L. Read,<sup>12</sup>  
 S. Reucroft,<sup>27</sup> M. Rijssenbeek,<sup>39</sup> T. Rockwell,<sup>23</sup> N.A. Roe,<sup>20</sup> P. Rubinov,<sup>39</sup> R. Ruchti,<sup>30</sup>  
 S. Rusin,<sup>24</sup> J. Rutherford,<sup>2</sup> A. Santoro,<sup>8</sup> L. Sawyer,<sup>42</sup> R.D. Schamberger,<sup>39</sup> H. Schellman,<sup>29</sup>  
 J. Sculli,<sup>26</sup> E. Shabalina,<sup>24</sup> C. Shaffer,<sup>13</sup> H.C. Shankar,<sup>41</sup> R.K. Shivpuri,<sup>11</sup> M. Shupe,<sup>2</sup>  
 J.B. Singh,<sup>32</sup> V. Sirotenko,<sup>28</sup> W. Smart,<sup>12</sup> A. Smith,<sup>2</sup> R.P. Smith,<sup>12</sup> R. Snihur,<sup>29</sup> G.R. Snow,<sup>25</sup>  
 S. Snyder,<sup>39</sup> J. Solomon,<sup>15</sup> P.M. Sood,<sup>32</sup> M. Sosebee,<sup>42</sup> M. Souza,<sup>8</sup> A.L. Spadafora,<sup>20</sup>  
 R.W. Stephens,<sup>42</sup> M.L. Stevenson,<sup>20</sup> D. Stewart,<sup>22</sup> D.A. Stoianova,<sup>33</sup> D. Stoker,<sup>5</sup> K. Streets,<sup>26</sup>  
 M. Strovink,<sup>20</sup> A. Taketani,<sup>12</sup> P. Tamburello,<sup>21</sup> J. Tarazi,<sup>6</sup> M. Tartaglia,<sup>12</sup> T.L. Taylor,<sup>29</sup>  
 J. Teiger,<sup>37</sup> J. Thompson,<sup>21</sup> T.G. Trippe,<sup>20</sup> P.M. Tuts,<sup>10</sup> N. Varelas,<sup>23</sup> E.W. Varnes,<sup>20</sup>  
 P.R.G. Virador,<sup>20</sup> D. Vititoe,<sup>2</sup> A.A. Volkov,<sup>33</sup> A.P. Vorobiev,<sup>33</sup> H.D. Wahl,<sup>13</sup> G. Wang,<sup>13</sup>  
 J. Wang,<sup>12,\*</sup> L.Z. Wang,<sup>12,\*</sup> J. Warchol,<sup>30</sup> M. Wayne,<sup>30</sup> H. Weerts,<sup>23</sup> F. Wen,<sup>13</sup> W.A. Wenzel,<sup>20</sup>  
 A. White,<sup>42</sup> J.T. White,<sup>43</sup> J.A. Wightman,<sup>17</sup> J. Wilcox,<sup>27</sup> S. Willis,<sup>28</sup> S.J. Wimpenny,<sup>7</sup>  
 J.V.D. Wirjawan,<sup>43</sup> J. Womersley,<sup>12</sup> E. Won,<sup>36</sup> D.R. Wood,<sup>12</sup> H. Xu,<sup>4</sup> R. Yamada,<sup>12</sup> P. Yamin,<sup>3</sup>  
 C. Yanagisawa,<sup>39</sup> J. Yang,<sup>26</sup> T. Yasuda,<sup>27</sup> C. Yoshikawa,<sup>14</sup> S. Youssef,<sup>13</sup> J. Yu,<sup>36</sup> Y. Yu,<sup>38</sup>  
 Y. Zhang,<sup>12,\*</sup> Y.H. Zhou,<sup>12,\*</sup> Q. Zhu,<sup>26</sup> Y.S. Zhu,<sup>12,\*</sup> Z.H. Zhu,<sup>36</sup> D. Zieminska,<sup>16</sup> A. Zieminski,<sup>16</sup>  
 and A. Zylberstejn<sup>37</sup>

<sup>1</sup> Universidad de los Andes, Bogotá, Colombia

<sup>2</sup> University of Arizona, Tucson, Arizona 85721

<sup>3</sup> Brookhaven National Laboratory, Upton, New York 11973

<sup>4</sup> Brown University, Providence, Rhode Island 02912

<sup>5</sup> University of California, Davis, California 95616

<sup>6</sup> University of California, Irvine, California 92717

<sup>7</sup> University of California, Riverside, California 92521

<sup>8</sup> LAFEX, Centro Brasileiro de Pesquisas Físicas, Rio de Janeiro, Brazil

<sup>9</sup> CINVESTAV, Mexico City, Mexico

<sup>10</sup> Columbia University, New York, New York 10027

<sup>11</sup> Delhi University, Delhi, India 110007

<sup>12</sup> Fermi National Accelerator Laboratory, Batavia, Illinois 60510

- <sup>13</sup>Florida State University, Tallahassee, Florida 32306  
<sup>14</sup>University of Hawaii, Honolulu, Hawaii 96822  
<sup>15</sup>University of Illinois at Chicago, Chicago, Illinois 60607  
<sup>16</sup>Indiana University, Bloomington, Indiana 47405  
<sup>17</sup>Iowa State University, Ames, Iowa 50011  
<sup>18</sup>Korea University, Seoul, Korea  
<sup>19</sup>Kyungshung University, Pusan, Korea  
<sup>20</sup>Lawrence Berkeley Laboratory and University of California, Berkeley, California 94720  
<sup>21</sup>University of Maryland, College Park, Maryland 20742  
<sup>22</sup>University of Michigan, Ann Arbor, Michigan 48109  
<sup>23</sup>Michigan State University, East Lansing, Michigan 48824  
<sup>24</sup>Moscow State University, Moscow, Russia  
<sup>25</sup>University of Nebraska, Lincoln, Nebraska 68588  
<sup>26</sup>New York University, New York, New York 10003  
<sup>27</sup>Northeastern University, Boston, Massachusetts 02115  
<sup>28</sup>Northern Illinois University, DeKalb, Illinois 60115  
<sup>29</sup>Northwestern University, Evanston, Illinois 60208  
<sup>30</sup>University of Notre Dame, Notre Dame, Indiana 46556  
<sup>31</sup>University of Oklahoma, Norman, Oklahoma 73019  
<sup>32</sup>University of Panjab, Chandigarh 16-00-14, India  
<sup>33</sup>Institute for High Energy Physics, 142-284 Protvino, Russia  
<sup>34</sup>Purdue University, West Lafayette, Indiana 47907  
<sup>35</sup>Rice University, Houston, Texas 77251  
<sup>36</sup>University of Rochester, Rochester, New York 14627  
<sup>37</sup>CEA, DAPNIA/Service de Physique des Particules, CE-SACLAY, France  
<sup>38</sup>Seoul National University, Seoul, Korea  
<sup>39</sup>State University of New York, Stony Brook, New York 11794  
<sup>40</sup>SSC Laboratory, Dallas, Texas 75237  
<sup>41</sup>Tata Institute of Fundamental Research, Colaba, Bombay 400005, India  
<sup>42</sup>University of Texas, Arlington, Texas 76019  
<sup>43</sup>Texas A&M University, College Station, Texas 77843

## INTRODUCTION

The Fermilab Tevatron Collider provides unique opportunity to study the properties of hard interactions in  $\bar{p}p$  collisions at short distances. The hard scattering is described by the theory of perturbative Quantum Chromodynamics (QCD) [1-3] and has been studied extensively in the last decade [4,5]. Within the context of QCD, the hard process is described as a point-like scattering between constituent partons (quarks and gluons) of protons and anti-protons. The scattering cross sections can be written in expansions of the strong coupling constant  $\alpha_s$ , convoluted with parton momentum distributions inside the nucleon. The lowest order  $\alpha_s^2$  term corresponds to the production of two-parton final states. Terms of order  $\alpha_s^3$  and  $\alpha_s^4$  in the expansion imply the existence of the three- and four-parton final states, respectively. Colored partons from the hard scattering evolve via soft quark and gluon radiation and hadronization processes to form observable colorless hadrons, which appear in the detector as localized energy deposits identified as jets. Jets originating from partons in the initial hard scattering process are typically isolated from other collision products and have large transverse energies. They are expected to preserve the energy and direction of the initial partons, and therefore the topologies of the final jet system are assumed to be directly related to those of the initial parton system.

The cross section and angular distributions for two-jet events have been successfully compared with the predictions of QCD [5,6]. A study of three- and four-jet events allows one to test the validity of QCD calculations to higher order ( $\alpha_s^3$  or beyond) and to probe the underlying QCD dynamics. This paper explores the topological distributions of three- and four-jet events. The distributions provide sensitive tests of the QCD matrix element calculations. Topological distributions for the three- and four-jet events have been published previously by the UA1, UA2 and CDF Collaborations [7–9]. However, all these studies imposed cuts on topological variables themselves, and therefore significantly reduced the phase space under study. This paper extends these studies to previously untested regions of phase space for a large number of topological variables. The measured normalized distributions, without restrictions on the topological variables themselves, are compared with QCD tree-level matrix element calculations. The predictions from simple phase-space matrix elements are also shown as a comparison, and the distributions of QCD subprocesses involving different number of quarks are examined.

### DEFINITION OF TOPOLOGICAL VARIABLES

The topological variables used in this paper are defined in the parton or jet center-of-mass system (CMS). The definitions refer to partons and jets interchangeably. The partons are assumed to be massless and the jet masses are ignored by using the measured jet energies as the magnitudes of jet momenta.

The topological properties of the three-parton final state in their center-of-mass system can be described in terms of six variables. Three of the variables define how the CMS energy is shared among the three final-state partons. The other three variables define the spatial orientation of the planes containing the three partons. It is convenient to introduce the notation:  $1 + 2 \rightarrow 3 + 4 + 5$  for the three-parton process. Here, numbers 1 and 2 refer to incoming partons while the numbers 3, 4 and 5 label the outgoing partons, ordered in descending CMS energies, i.e.  $E_3 > E_4 > E_5$ . The final state parton energies are obvious choices for the topological variables. For simplicity,  $E_i (i = 3, 4, 5)$  are often replaced by the scaled variables  $x_i (i = 3, 4, 5)$ , which are defined by  $x_i = 2E_i/\sqrt{\hat{s}}$ , where  $\sqrt{\hat{s}}$  is the center-of-mass energy of the hard process. By definition,  $x_3 + x_4 + x_5 = 2$ . It is worth noting that the scaled parton energies ( $x_i, i = 3, 4, 5$ ) and the angles between partons ( $\omega_{jk}, j, k = 3, 4, 5$ ) for the three-parton final state have the following relationship:

$$x_i = \frac{2 \sin \omega_{jk}}{\sin \omega_{34} + \sin \omega_{45} + \sin \omega_{53}}, \quad (1)$$

where  $i, j, k = 3, 4, 5$  and  $i \neq j \neq k$ . Clearly, the internal structure of the three-parton final state is completely determined by any two scaled parton energies. The angles that fix the event orientation can be chosen to be: (1) the cosine<sup>2</sup> of the polar angle with respect to the beam ( $\cos^2 \theta_3^*$ ), (2) the azimuthal angle ( $\phi_3^*$ ) of parton 3, and (3) the angle ( $\psi^*$ ) between the plane containing partons 1 and 3 and the plane containing partons 4 and 5 defined by:

$$\cos \psi^* = \frac{(\vec{p}_1 \times \vec{p}_3) \cdot (\vec{p}_4 \times \vec{p}_5)}{|\vec{p}_1 \times \vec{p}_3| |\vec{p}_4 \times \vec{p}_5|}, \quad (2)$$

where  $\vec{p}_i (i = 1, \dots, 5)$  is the parton momentum. For unpolarized beams (as they are at Tevatron), the  $\phi_3^*$  distribution is uniform. Therefore, only four independent kinematic

---

<sup>2</sup>Unless otherwise specified, the absolute values on the cosines of polar angles are implied throughout this paper.

variables are needed to describe the topological properties of the three-parton final state. In this paper, they are chosen to be  $x_3, x_5, \cos \theta_3^*$  and  $\psi^*$ . Using dimensionless variables and making comparisons on normalized distributions sidesteps many issues of detector resolution and energy scale and therefore allows a direct comparison between data and theoretical calculation.

Other variables of interests are scaled invariant masses of jet pairs:

$$\mu_{ij} = \frac{m_{ij}}{\sqrt{\hat{s}}} \equiv \sqrt{x_i x_j (1 - \cos \omega_{ij})/2} \quad i, j = 3, 4, 5 \quad \text{and} \quad i \neq j, \quad (3)$$

where  $m_{ij}$  is the invariant mass of partons  $i$  and  $j$  and  $\omega_{ij}$  is the opening angle between the two partons. The scaled invariant mass ( $\mu_{ij}$ ) is sensitive to the scaled energies of the two partons, the angle between the two partons and the correlations between these variables.

The four-parton final state is more complicated. Apart from the CMS energy, eight independent parameters are needed to completely define a four-parton final state in its center-of-mass system. Two of these define the overall event orientation while the other six fix the internal structure of the four-parton system. In contrast to the three-parton final state, there is no simple relationship between the scaled parton energies and the opening angles between partons. Consequently, the choices of topological variables are less obvious in this case. In this paper, we define variables in a similar way to those investigated for the three-parton final state. Four partons are ordered in descending CMS energy and labeled from 3 to 6. The variables we study include the scaled energies ( $x_i, i = 3, \dots, 6$ ) and the cosines of polar angles ( $\cos \theta_i^*, i = 3, \dots, 6$ ) of the four jets, the cosines of the angles ( $\cos \omega_{ij} \quad i, j = 3, \dots, 6$  and  $i \neq j$ ) and the scaled masses ( $\mu_{ij} = m_{ij}/\sqrt{\hat{s}} \quad i, j = 3, \dots, 6$  and  $i \neq j$ ) of partons. In addition, two variables characterizing the orientations of event planes are investigated. One of the two variables is the ‘Bengtsson-Zerwas’ angle ( $\chi_{BZ}$ ) [10] defined as the angle between the plane containing two leading jets and the plane containing two non-leading jets:

$$\cos \chi_{BZ} = \frac{(\vec{p}_3 \times \vec{p}_4) \cdot (\vec{p}_5 \times \vec{p}_6)}{|\vec{p}_3 \times \vec{p}_4| |\vec{p}_5 \times \vec{p}_6|}. \quad (4)$$

The other variable is the cosine of ‘Nachtmann-Reiter’ angle ( $\cos \theta_{NR}$ ) [11] defined as the angle between the momentum vector differences of the two leading jets and the two non-leading jets:

$$\cos \theta_{NR} = \frac{(\vec{p}_3 - \vec{p}_4) \cdot (\vec{p}_5 - \vec{p}_6)}{|\vec{p}_3 - \vec{p}_4| |\vec{p}_5 - \vec{p}_6|}. \quad (5)$$

Historically, the  $\chi_{BZ}$  and  $\cos \theta_{NR}$  were proposed for  $e^+e^-$  collisions to study the gluon self-coupling. The situation in  $\bar{p}p$  collisions is much more complicated. The variables are used as a tool for studying the internal structure of the four-jet events.

## THE THEORETICAL MODEL

The cross section for the production of the  $n$ -parton final state  $1 + 2 \rightarrow 3 + \dots + (n + 2)$ , in  $\bar{p}p$  collisions at a center-of-mass energy,  $\sqrt{s}$ , is described by the following expression:

$$\sigma_n = \sum_{\ell} \int f_1^{\ell}(x_1) f_2^{\ell}(x_2) |M_{\ell}^n|^2 \Phi_n dx_1 dx_2, \quad (6)$$

where  $\sum_{\ell}$  sums over all possible  $1 + 2 \rightarrow n$ -parton subprocesses.  $f_1^{\ell}(x_1)$  and  $f_2^{\ell}(x_2)$  are the parton density distributions of incoming partons.  $|M_{\ell}^n|^2$  represents for the matrix elements of the subprocess and  $\Phi_n$  is the  $n$ -body phase space. In general, to the lowest order  $|M_{\ell}^n|^2 \propto \alpha_s^n / \sqrt{\hat{s}}$  with  $\hat{s} = x_1 x_2 s$ . Theoretically  $|M_{\ell}^n|^2$  is well behaved if calculated to all orders in the  $\alpha_s$  expansion. At present, this calculation is technically not possible. Therefore one has to deal with truncated matrix elements in the  $\alpha_s$  expansion. As a result,  $|M_{\ell}^n|^2$  diverges when the energy of any final state parton or the angle between any two partons approaches zero. The singularities in  $|M_{\ell}^n|^2$  cause poles in the topological distributions. In comparison, a phase space model in which  $|M_{\ell}^n|^2 \propto 1/\hat{s}^{n-2}$  does not have singularities in the matrix element. In this paper, the distributions from the phase space model are used as references for the comparisons between the data and QCD.

The straight-forward approach for modelling perturbative QCD for multi-jet production is the matrix element method, in which Feynman diagrams are calculated order by order in  $\alpha_s$ . Technical difficulties have limited the calculations to the tree-level of the relevant processes. The exact tree-level matrix element calculation for the three-parton final state has been available for some time [12]. The complete tree-level matrix element calculations for up to five final state partons have been recently calculated by Berends-Giele-Kuijf (BGK) [13] using a Monte Carlo method. The other commonly used approximate calculations are those of Kunszt-Stirling (KS) [14] and of Maxwell [15]. The perturbative QCD calculations have been incorporated into several partonic event generators. For the analysis described in this paper, the NJETS [13] program is used to calculate QCD predictions while the PAPAGENO [16] program is used as a cross check and to calculate distributions from the phase space model. The exact tree-level matrix elements calculations for up to five jets are implemented in the NJETS program. PAPAGENO implements an exact matrix element calculation of tree-level contributions for final states with up to three outgoing partons and provides Kunszt-Stirling and Maxwell approximations to six outgoing partons. These approximations are used in part to speed up the calculations, in view of the complicated exact matrix elements.

## THE DATA SAMPLE

The data used in this analysis was collected with the DØ detector during the 1992-1993 Tevatron run at a center-of-mass energy of 1800 GeV. The DØ detector consists of a central tracking system, a calorimeter and muon chambers. Jets are measured in the calorimeter, which has a transverse segmentation of  $\Delta\eta \times \Delta\phi = 0.1 \times 0.1$ . The jet energy resolution has been determined to be 13% at 50 GeV and 7% at 150 GeV. The jet direction is measured to better than 0.05 in both  $\eta$  and  $\phi$ . With the hermetic and uniform rapidity coverage ( $-4.5 < \eta < 4.5$ ) of the calorimeter, the DØ detector is especially suited for studying multi-jet physics. The detailed description of the DØ detector can be found elsewhere [17].

The events used in this study passed hardware (Level 1) and software (Level 2) cluster-based triggers. In addition, a Level 0 trigger required that vertices along the beam line be within 10.5 cm of  $z = 0$ . The Level 1 trigger was based on calorimeter energy deposited in towers of size  $\Delta\eta \times \Delta\phi = 0.2 \times 0.2$ . The events were required to have at least two such towers with registered transverse energy ( $E_T$ ) above 7 GeV. The successful candidates were passed to the Level 2 trigger, which sums transverse energies of calorimeter towers within a radius of  $\mathcal{R}(\equiv (\Delta\eta^2 + \Delta\phi^2)^{1/2}) = 0.7$ . The Level 2 trigger selected those events with at least one such cone, built around the Level 1 trigger tower, with transverse energy above 50 GeV. The total effective luminosity used in this analysis is  $1.2 \text{ pb}^{-1}$ . The trigger efficiency for events with at least one jet with  $E_T > 60 \text{ GeV}$  is above 90%. A detailed description of the

trigger can be found elsewhere [18].

The offline reconstruction uses a fixed-cone jet algorithm with  $\mathcal{R} = 0.7$ , similar to the algorithm used in the Level 2 trigger. The jet reconstruction begins with seed calorimeter towers of size  $\Delta\eta \times \Delta\phi = 0.1 \times 0.1$  with more than 1 GeV transverse energy. Towers are represented by massless four-momentum vectors with directions given by the tower positions and event vertices. The four momenta of towers in the cone around the seed tower are summed to form the four-momentum vector of the jet. The jet direction is then recalculated using tower directions weighted by their transverse energies. The procedure is repeated until the jet axis converges. The final jet  $E_T$  is the sum of the transverse energies of towers within the cone, while the jet direction is determined by the jet four-momentum vector  $(E, E_x, E_y, E_z)$ , i.e.,  $\theta = \cos^{-1}(E_z/\sqrt{E_x^2 + E_y^2 + E_z^2})$ ,  $\phi = \tan^{-1}(E_y/E_x)$  and  $\eta = -\ln \tan(\theta/2)$ .

The jet energies have been calibrated using direct photon candidates by balancing jet  $E_T$  against that of the photon candidate. The electromagnetic energy scale is determined by comparing the measured electron pair mass of  $Z \rightarrow e^+e^-$  events with the  $Z$  mass [19] measured by  $e^+e^-$  experiments. The calibration takes into account the effects of out-of-cone showering using shower profiles from test beam as well as the underlying event using events from the minimum-bias trigger. Details can be found in ref. [20].

After the energy corrections, jets are required to have  $E_T$  greater than 20 GeV and lie within pseudorapidity range  $-3.0$  to  $3.0$ . The pseudorapidity is calculated with respect to the event vertex determined from tracks measured by the central tracking detector. Jets passing the above cuts are ordered in decreasing order of  $E_T$ . The  $E_T$  of the leading jet must be greater than 60 GeV to reduce possible trigger bias.

Three-jet events are selected by further demanding that there be at least three jets. This leaves about 94,000 events in the sample. The separation between jets ( $\Delta\mathcal{R}$ ) in  $\eta \times \phi$  space is required to be greater than 1.4, which is twice the cone size used, to avoid merging/splitting problems associated with the cone jet algorithm. This requirement removes events with overlapping jets and therefore ensures good jet energy and direction measurements. Approximately 70% of the events passed this cut. The invariant mass distribution of the three highest  $E_T$  jets is shown in Fig. 1. Also shown is the distribution from the exact tree-level calculations of the perturbative QCD. The overall agreement between the data and the QCD distributions is good with the exception of the low mass region. To reduce possible bias in the turn-on, the invariant mass of the three leading jets is required to be above 200 GeV. After all cuts, a sample of  $\sim 46,000$  three-jet events remains. The surviving events are then transformed to the CMS frame of the three leading jets. Any other jets in the event are ignored. The jets are then re-ordered in descending energy in their CMS system. The topological variables ( $x_3, x_4, \cos\theta_3^*$  and  $\psi^*$ ) are calculated. Unlike previous studies by other experiments, no cuts on these topological variables are imposed.

Four-jet events are selected in a similar manner. Events are required to have at least four jets, which results in a data sample of 19,000 events. The distance between any jet pair in  $\eta \times \phi$  plane is required to be greater than 1.4, reducing the data sample further to about 8,400 events. As in the selection of the three-jet events, the invariant mass of the leading four jets must be above 200 GeV. A total 8,100 events remain in the four-jet event sample. The four leading jets of the remaining events are boosted to their center-of-mass system. Additional jets, if present, are ignored. The boosted jets are then ordered in decreasing energy. The topological variables are calculated using the four boosted momentum vectors after ordering in decreasing energy. No cuts on the topological variables are imposed.

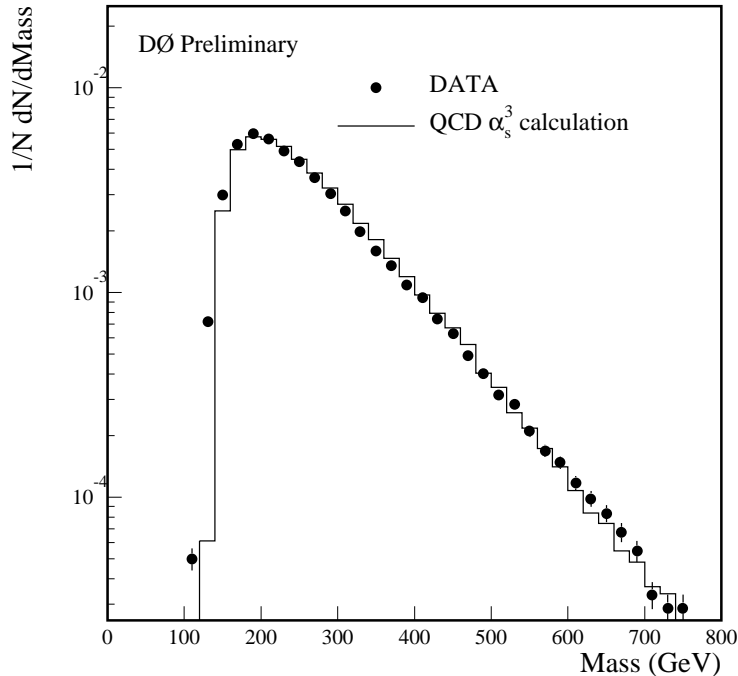


**FIG. 1.** The normalized mass distribution of the three highest  $E_T$  jets of the selected three-jet events before the mass cut.

### PREDICTIONS OF THEORETICAL MODELS

The partonic event generator NJETS is used to calculate the exact tree-level QCD distributions. The PAPAGENO program is used to calculate the distributions of the phase space model as well as the approximate calculations of Kunszt-Stirling [14]. Unless otherwise specified, the parton density function used in the calculations is MRS (BCDMS fit) [21] for both NJETS and PAPAGENO. The QCD scale parameter is set to 200 MeV and the renormalization scales are set to the average transverse momentum of the outgoing partons for both matrix elements and parton density functions. The outgoing partons are analyzed as if they were observed jets and the selection criteria described above are applied to select three- and four-jet events.

To study the sensitivity on the choice of parton density function, the topological distributions of QCD calculations with different parton density functions are compared. For NJETS, the comparisons are made between MRS [21] and EHLQ [22] parton density functions. For PAPAGENO the parton density functions of MRS [21] and Morfin-Tung [23] are employed. Although the total three- and four-jet cross sections vary as much as 30% for different parton density functions, the normalized topological distributions are found to be very insensitive to the choice. A typical difference of less than 3% is found for the variables studied. The dependences on the renormalization scale are investigated using the PAPAGENO program. The distributions for the renormalization scales of (1) average transverse momentum, (2)

one half average value of transverse momentum and (3) total transverse energy are compared. Despite large differences (as much as 60%) in the total production cross sections, the differences between normalized distributions are very small, typically less than 3%.

The fragmentation effect is investigated using the HERWIG 5.8 [24] event generator. The parton-level distributions are compared with the distributions at particle level. The differences between the distributions before and after fragmentation are found to be small, typically at the 4% level. Combining all the effects described above, the total uncertainty on the theoretical predictions is 6%.

Both NJETS and PAPAGENO incorporate tree-level calculations for three- and four-parton final states. The effect on the normalized distributions due to higher order loop corrections is expected to be small in the phase space region relevant to the analyses described in this paper [25]. They generate exclusive three- or four-parton events. On the other hand, it is not possible to select a data sample which corresponds to tree-level diagrams. As described above, inclusive three- or four-jet events are selected. In this paper, the data distributions based on the inclusive samples are compared with the QCD calculations from exclusive final states.

## UNCERTAINTIES OF THE MEASURED TOPOLOGICAL DISTRIBUTIONS

The measured distributions of topological variables are affected by detector effects: (a) the limited trigger efficiency, (b) the detector acceptance and resolution and (c) the uncertainty of the energy scale. However, most of these corrections and their uncertainties are minimized by normalizing the distributions to unity. In the following, residual uncertainties are investigated.

The non-uniformity of the detector acceptance and of the trigger efficiency in the topological variables and the imperfect detector energy resolution and angular resolution have direct effects on the measured distributions. These effects are estimated using a fast detector simulation program which takes into account the detector energy and angular resolution and the trigger efficiency as functions of the pseudorapidity and the transverse energy of jets. The bin-by-bin correction factors are flat within 5%, apart from some low statistics bins which vary up to 10%.

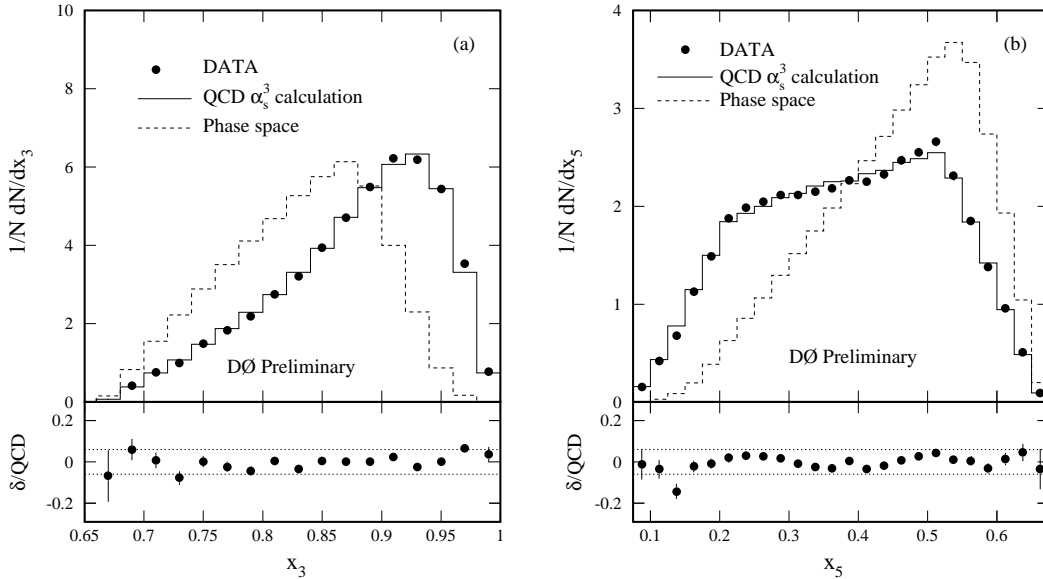
By definition, the topological variables have a weak dependence on the energy scale since only the scaled energies and directions of the jets are used. However, the event selection criteria, such as  $E_T$  and invariant mass cuts, are vulnerable to energy scale error. The possible distortion of the measured topological variables due to the uncertainty in the energy scale is studied by varying the energy calibration constants within their nominal errors. The selection procedure described above is repeated on the events calibrated with these modified constants. Apart from some low statistics bins, the variations in the measured topological variables are very small. We conservatively assign a 3% systematic error on the topological distributions due to energy scale uncertainty. The small variation is in part due to the fact that the topological distributions change slowly with the jet  $E_T$  and the invariant mass of the jet system.

In principle, the measured distributions have to be corrected for detector effects before the data can be compared with the theoretical calculations. However, adding the above systematic effects in quadrature, we get a 6% uncertainty on the measured distributions. The small detector effects suggest that the data distributions can be directly compared with the parton-level distributions of perturbative QCD calculations, alleviating the need for time-consuming computer detector simulations. In the following, the measured distributions with a 6% estimated total systematic error are directly compared with the QCD tree-level

calculations at parton level.

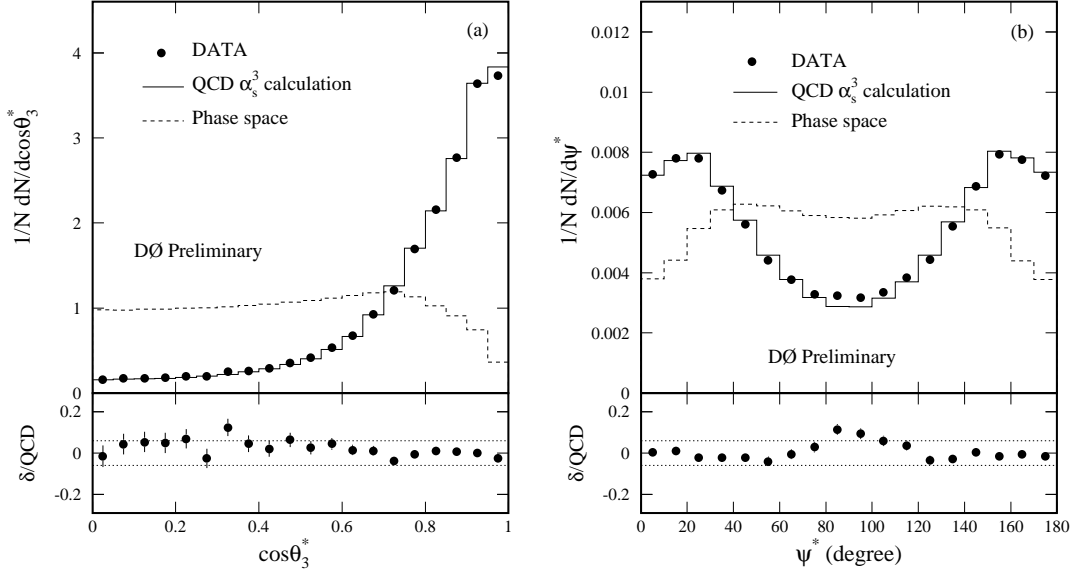
### THE TOPOLOGIES OF THREE-JET EVENTS

Figure 2 shows the measured  $x_3$  and  $x_5$  distributions for the final selection of three-jet events. The three jets are labeled in order of decreasing energy in their CMS frame. The average values of  $x_3$  and  $x_5$  are 0.88 and 0.39 respectively. The data are compared with the predicted distributions of the exact QCD tree-level calculations and the expectations from the phase-space model. The QCD calculations reproduce the measured distributions well for the whole range. Unlike the predictions of the phase-space model, the data heavily populate the high  $x_3$  region and have significant contributions at low  $x_5$  values, a characteristic of gluon radiation. The decrease in  $x_3$  distributions at high  $x_3$  values is due to the  $\Delta\mathcal{R}$  cut in the event selection. The bottom plot shows the fractional difference between the data and the QCD predictions with dotted lines indicating the estimated 6% systematic error on the measurement. The differences between the data and the predictions are within the systematic error band.



**FIG. 2.** The scaled energy distributions: (a)  $x_3$  and (b)  $x_5$  of the three-jet events in their center-of-mass system. Only statistical errors are shown. The bottom plot shows the fractional difference between the data and the exact tree-level QCD calculation. The dotted lines show the estimated 6% systematic uncertainty on the measurement.

The  $\cos\theta_3^*$  distribution is shown in Fig. 3(a). As in the angular distribution of two-jet events, an angular dependence characteristic of Rutherford  $t$ -channel scattering is unmistakable. The large angular coverage of the DØ calorimeter allows the analysis to cover the entire  $\cos\theta_3^*$  range, extending the study into a previously untested region of phase space. As is evident in the figure, the data are well reproduced by the predictions of the exact QCD tree-level calculations over the entire range of  $\cos\theta_3^*$ . The phase-space distribution is



**FIG. 3.** The distributions of (a) the cosine of the leading jet polar angle and (b) the angle between the plane defined by the leading jet and the beam line and the plane defined by two non-leading jets of the three-jet events in their center-of-mass system. The dotted lines show the estimated 6% systematic uncertainty on the measurement.

mostly flat with high  $\cos \theta_3^*$  bins suppressed as a result of the pseudorapidity cut in the event selection. The depletions in the data and the QCD calculations are compensated by a large cross section in this region and therefore are less visible. The measured  $\psi^*$  distribution is shown in Fig. 3(b) together with the results of the exact QCD tree-level calculation and of the phase-space model. The phase-space distribution shows depletions at small and large  $\psi^*$  angles, an effect of the event selection. However, the data and the QCD distributions are enhanced in these regions because of the initial-state radiation in which one of the two non-leading jets is close to the beam line. As in the case of the  $x_3$ ,  $x_5$  and  $\cos \theta_3^*$  distributions, the overall agreement between data and the QCD tree-level calculations is very good.

The scaled mass distributions are sensitive to the jet energies, the opening angles between jets and the correlations between these quantities. The measured  $\mu_{34}$ ,  $\mu_{35}$  and  $\mu_{45}$  distributions for the three-jet event sample are compared with the exact QCD predictions in Fig. 4. The QCD predictions agree with the data well while the differences between the data and the phase-space model are large.

Finally, we note that the KS approximate QCD calculations are essentially identical to the exact tree-level QCD calculations for the topological variables studied above. This implies that the topological distributions are insensitive to the approximation made in the calculations.

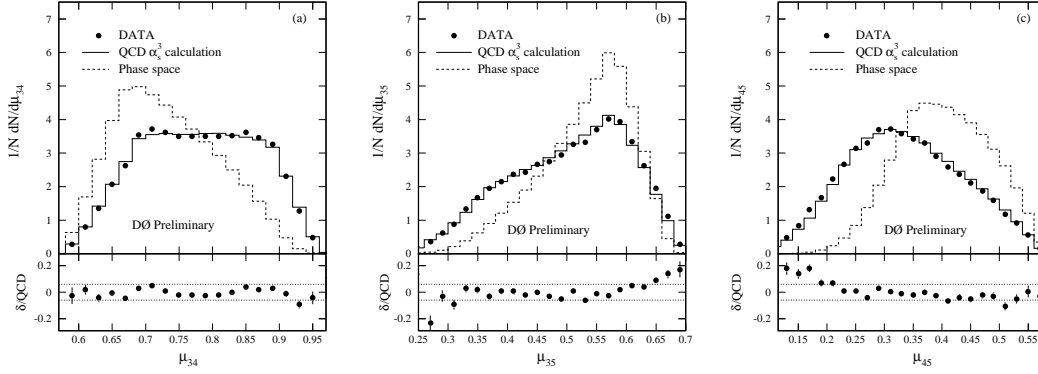


**FIG. 4.** The scaled mass distributions: (a)  $\mu_{34}$ , (b)  $\mu_{35}$  and (c)  $\mu_{45}$  of the three-jet events in their center-of-mass system. The bottom plots show fractional differences between the data and QCD. The dotted lines show the 6% systematic uncertainty on the measurement.

## THE TOPOLOGIES OF FOUR-JET EVENTS

The four measured energy fractions of four-jet events are shown in Fig. 5. The four jets are labeled in order of decreasing energy in their center-of-mass system. Although four scaled energy variables are shown, only three of these are independent. The other one is fixed by the condition  $\sum_i x_i = 2$ . The measured mean values of four energy fractions are 0.76, 0.61, 0.39 and 0.24. The QCD predictions of the exact tree-level calculations are represented by the solid curves and are in an excellent agreement with the data for all four variables. As in the three-jet case, the distributions from the phase-space model do not reproduce the data. The fractional differences between the data and QCD are very similar to those of the three-jet events and are not shown for simplicity.

The cosines of the four polar angles of the four-jet events in their center-of-mass system are compared with QCD calculations in Fig. 6 for the entire range. While the two leading jets tend to be in the forward region, the cosine distribution of the least energetic jet is essentially flat, because the  $\Delta\mathcal{R}$  cut in the event selection favors events with other jets in central region. Although small differences between the data and the QCD calculations are visible, the overall agreement is good. Despite the large differences between the data and the phase-space model in  $\cos\theta_3^*$  and  $\cos\theta_4^*$  distributions, the differences in the other two distributions are relatively small.

The internal event structure can be further understood by examining the opening angles between jets. Figure 7 shows the distributions of angle between all possible jet pairs of the four-jet events in their center-of-mass system. While the two leading jets are mostly back-to-back, the angles between other jet pairs distribute widely. The depletions in regions of  $\cos\omega_{ij} \rightarrow 1.0$  are again due to the  $\Delta\mathcal{R}$  cut in the event selection. The structures of the data distributions are well described by the QCD predictions.

Figure 8 shows the scaled mass distributions of jet pairs of the four-jet events for both data and the QCD calculations. The average scaled mass is 0.65 for two leading jets and is 0.23 for two non-leading jets. The QCD calculations agree with the data well. Distributions of the phase-space model are generally too narrow and fail to reproduce the data distributions.

Figure 9 compares the measured  $\chi_{BZ}$  and  $\cos\theta_{NR}$  distributions with the predictions of

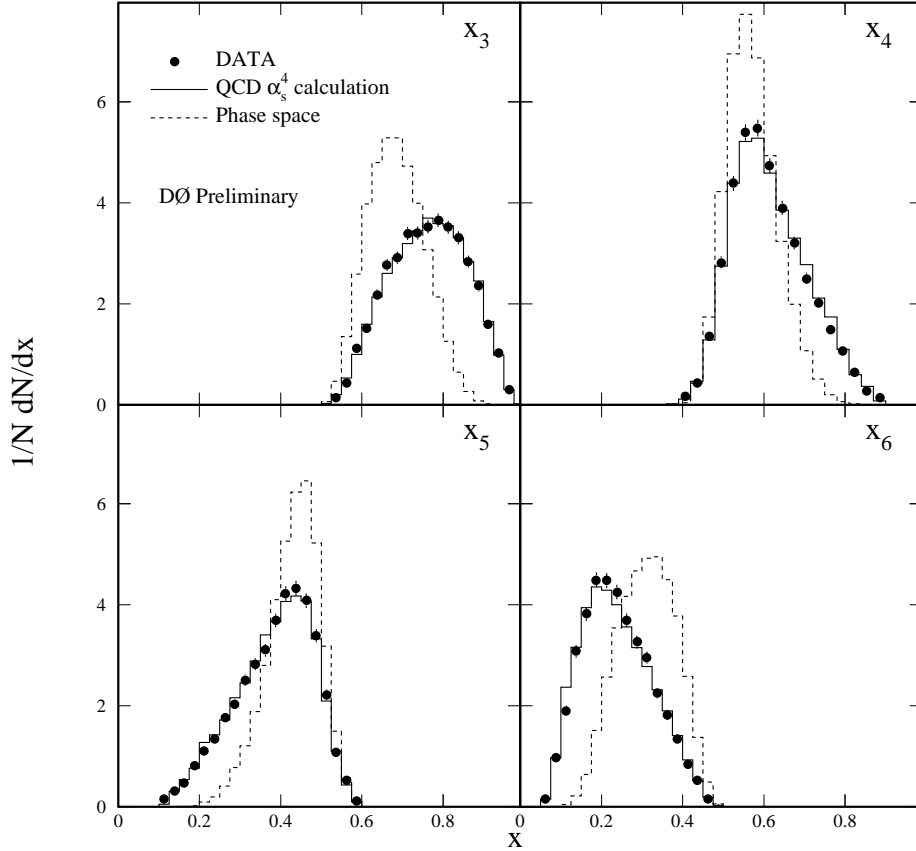


**FIG. 5.** The four energy fractions of the four-jet events in their center-of-mass system. Only statistical errors are shown. The estimated systematic uncertainty on the measurement is 6%.

the exact tree-level QCD calculations as well as those from the phase space model. The agreement between the data and QCD predictions is generally good and the differences between the data and the phase space model are large. Although the jet separation cut in the event selection favors large  $\chi_{BZ}$ , the data and the QCD distributions have significant contributions in small  $\chi_{BZ}$  angle region, which corresponds to a planar topology of the four jets. In contrast, the phase space distribution is highly suppressed in this region. The  $\cos\theta_{NR}$  distributions for the data and QCD are essentially flat while it peaks strongly as  $\cos\theta_{NR}$  approaches 0 for the phase space model.

For the four-jet events as for the three-jet events, although not shown the normalized distributions from the KS approximate QCD calculations agree well with the data.

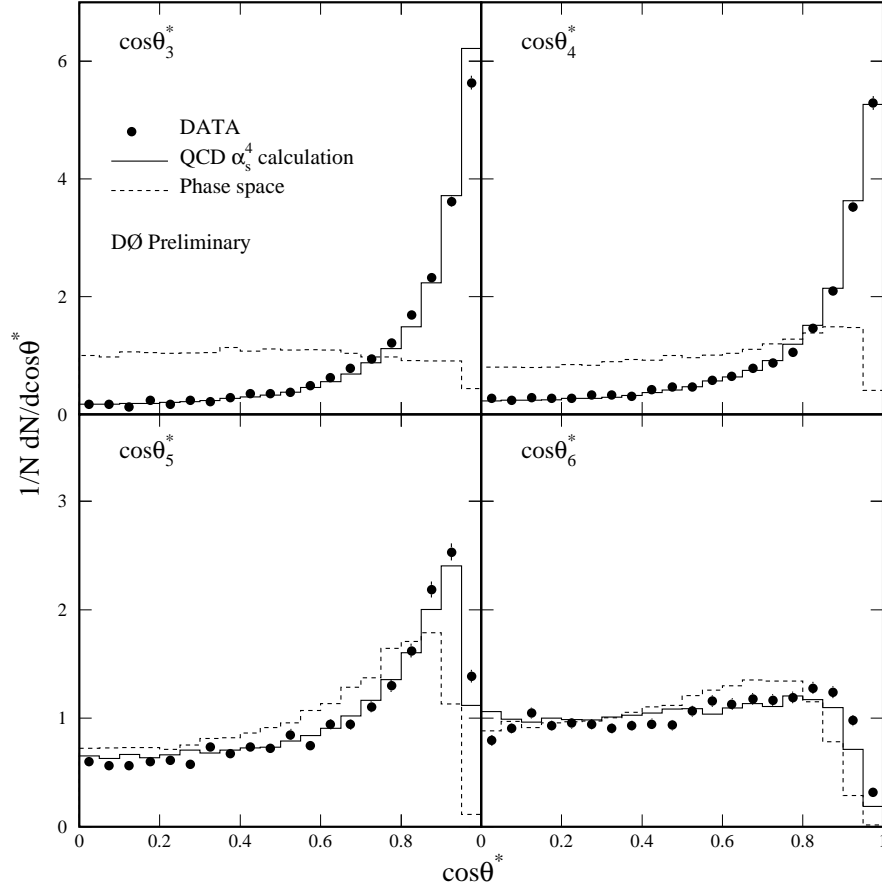


**FIG. 6.** The four cosines of polar angle of the four-jet events in their center-of-mass system. Only statistical errors are shown. The estimated systematic uncertainty on the measurement is 6%.

### COMPARISON OF QCD SUBPROCESSES

At the parton level, five and six partons (including two initial partons) are involved in the three- and four-jet processes respectively. While it is difficult, if not impossible, to label quark or gluon jets in the data, the three-jet process can be broken into three subprocesses involving different numbers of quarks with the partonic NJETS and PAPAGENO event generators: (1) 0-quark, (2) 2-quark and (3) 4-quark. The predicted fractional contributions by NJETS to the total three-jet cross section for the cuts described above are 32.9%, 50.8% and 16.2% for 0-quark, 2-quark and 4-quark subprocesses respectively. Similarly, the four-jet process can be divided into (1) 0-quark (29.4%), (2) 2-quark (49.6%), (3) 4-quark (20.2%) and (4) 6-quark (0.7%) subprocesses.

The studies described above show that the QCD calculations agree well with the data. It is therefore interesting to examine the topological distributions of these subprocesses. Figure 10 (a) and (b) show the  $x_4$  and  $\cos\theta_4^*$  distributions of the three-jet events and Fig. 10 (c) and (d) show the  $x_5$  and  $\cos\theta_5^*$  distributions of the four-jet events predicted by the

exact tree-level QCD calculations (full QCD) and by the QCD calculations of the three subprocesses. The full QCD is normalized to unity and the subprocesses are normalized to the fractional contributions to their respective total cross section quoted above. The data distributions are normalized to the respective QCD distributions. The distributions of the subprocesses are remarkably similar and agree well with the data. The 6-quark subprocess contributes less than 1% of the total cross section of the four-jet events and therefore is not shown in Fig. 10 (c) and (d). Nevertheless, the normalized distributions are very similar to those of other three subprocesses. The similarity of the subprocesses is observed in all other variables of the three- and four-jet events investigated in this paper. The observation suggests that the distributions are insensitive to the relative contributions of these subprocesses to the total cross section and implies that the distributions are largely determined by the matrix elements and have weak dependences on the quark-gluon content in parton density functions. Therefore, the comparisons between measured and predicted distributions provide direct tests of the validity of the matrix element calculations. Furthermore, Rutherford characteristics are visible in  $\cos\theta^*$  distributions for all subprocesses, implying that the matrix elements of these subprocesses are dominated by the  $t$ -channel gluon exchange.

### SUMMARY

From the data sample recorded by the  $D\bar{D}$  detector in  $\bar{p}p$  collisions at  $\sqrt{s} = 1800$  GeV at the Tevatron during the 1992-1993 running period, high statistics three-jet and four-jet event samples have been selected. A large number of distributions characterizing the global structures of the three- and four-jet events have been compared with QCD calculations of the exact tree-level matrix elements and with calculations of the QCD subprocesses involving different numbers of quarks. All comparisons have been made with the parton-level calculations and based on normalized distributions rather cross sections.

For the three-jet events, the investigated topological variables are: energy fractions carried by the two leading jets, the cosine of the leading jet polar angle, the angle between the plane containing the leading jet and beam line, the plane containing the two non-leading jets, and the scaled invariant masses of between the jets. In the case of the four-jet events, the energy fractions and the cosines of the polar angles of all four jets, the six opening angles, scaled invariant masses between the jets and the angles between jet planes have been studied.

Studies show that the measured topological distributions of the three- and four-jet events are well reproduced by the exact tree-level matrix elements QCD calculations. The good agreement implies that the topological distributions of the three- and four-jet events are determined by the tree-level diagrams and therefore the topological distributions are not very sensitive to higher order corrections. Furthermore, the distributions are found to be insensitive to the uncertainties in parton density functions and to the quark/gluon flavor of underlying partons. The dominance of the  $t$ -channel gluon exchange to a large extent determines the structure of the event. The successful direct comparison between the data and the QCD calculations at the parton level reaffirms the assumption that jets follow closely their underlying partons at high energies. The differences between the data and the phase space model are large for most of the distributions.

### ACKNOWLEDGMENTS

We thank the Fermilab Accelerator, Computing, and Research Divisions, and the support staffs at the collaborating institutions for their contributions to the success of this work. We also acknowledge the support of the U.S. Department of Energy, the U.S. National

Science Foundation, the Commissariat à l'Énergie Atomique in France, the Ministry for Atomic Energy and the Ministry of Science and Technology Policy in Russia, CNPq in Brazil, the Departments of Atomic Energy and Science and Education in India, Colciencias in Colombia, CONACyT in Mexico, the Ministry of Education, Research Foundation and KOSEF in Korea and the A.P. Sloan Foundation.

## REFERENCES

- \* Visitor from IHEP, Beijing, China.
  - † Visitor from CONICET, Argentina.
  - § Visitor from Universidad de Buenos Aires, Argentina.
  - ¶ Visitor from Univ. San Francisco de Quito, Ecuador.
1. M. Gell-Mann, *Acta Physica Austriaca*, Suppl. **IX** (1972) 733;  
H. Fritzsch and M. Gell-Mann, 16th International Conference on High Energy Physics, Batavia, 1972; editors J.D. Jackson and A. Roberts, National Accelerator Laboratory (1972);  
H. Fritzsch, M. Gell-Mann and H. Leytwyler, *Phys. Lett.* **B47** (1973) 365.
  2. D.J. Gross and F. Wilczek, *Phys. Rev. Lett.* **30** (1973) 1343; *Phys. Rev.* **D8** (1973) 3633;  
H.D. Politzer, *Phys. Rev. Lett.* **30** (1973) 1346.
  3. G. 't Hooft, *Nucl. Phys.* **B33** (1971) 173.
  4. For recent reviews on QCD tests at  $e^+e^-$  collider see:  
S. Bethke, J.E. Pilcher, *Ann. Rev. Nucl. Part. Sci.*, **42** (1992) 251;  
T. Hebbeker, *Phys. Rep.* **217** (1992) 69.
  5. For recent reviews on QCD tests at  $\bar{p}p$  collider see:  
J.E. Huth and M.L. Mangano, *Ann. Rev. Nucl. Part. Phys.*, **43** (1993) 585;  
R.K. Ellis and W.J. Stirling, Fermilab preprint, Fermilab-Conf-90/164-T (1990).
  6. DØ Collaboration, S. Abachi *et al.*, DØ note #1829.
  7. UA1 Collaboration, G. Arnison *et al.*, *Phys. Lett.* **B158** (1985) 494;  
UA2 Collaboration, J.A. Appel *et al.*, *Z. Phys.* **C30** (1986) 341;  
CDF Collaboration, F. Abe *et al.*, *Phys. Rev.* **D45** (1992) 1448.
  8. UA2 Collaboration, J. Alitti *et al.*, *Phys. Lett.* **B268** (1991) 145.
  9. CDF Collaboration, F. Abe *et al.*, Fermilab Preprint, Fermilab-Pub-93/003-E (1993).
  10. M. Bengtsson and P.M. Zerwas, *Phys. Lett.* **B208** (1988) 306.
  11. O. Nachtmann and A. Reiter, *Z. Phys.* **C16** (1982) 45.
  12. Z. Kunszt and E. Pietarinen, *Nucl. Phys.* **B164** (1980) 45;  
T. Gottschal and D. Sivers, *Phys. Rev.* **D21** (1980) 102;  
F.A. Berends *et al.*, *Phys. Lett.*, **B118** (1981) 124.
  13. F.A. Berends, W.T. Giele and H. Kuijf, *Nucl. Phys.* **B333** (1990) 120; *Phys. Lett.* **B232** (1990) 266.
  14. Z. Kunszt and W.J. Stirling, *Phys. Lett.* **B171** (1986) 307; *Phys. Rev.* **D56** (1988) 2439.
  15. C.J. Maxwell, *Phys. Lett.* **B192** (1987) 190; *Nucl. Phys.* **B316** (1989) 321;  
M.L. Mangano and S.J. Parke, *Phys. Rev.* **D39** (1989) 758;  
C.J. Maxwell and S.J. Parke, *Phys. Rev.* **D44** (1991) 2727.
  16. I. Hinchliffe, LBL preprint, LBL-34372 (July 1993).
  17. S. Abachi *et al.* (The DØ Collaboration), *Nucl. Instrum. Meth.* **A338** (1994) 185.
  18. J. Linnemann, in proceedings of the 7th Meeting of the APS Division of Particles and Fields, Batavia (1992);  
R. Astur and A. Milder, DØ note #1663.
  19. Particle Data Group, K. Hikasa *et al.*, *Phys. Rev.* **D45** (1992) II.1.
  20. J. Kotcher, in proceedings of the 1994 Beijing Calorimetry Symposium, IHEP - Chinese Academy of Sciences, Beijing, China, Oct. 25-27, 1994 (to be published).

- H. Weerts, in proceedings of *9th Topical Workshop on Proton-Antiproton Collider Physics*, edited by K. Kondo and S. Kim, (Universal Academy Press, Tokyo, Japan, 1994).
21. A.D. Martin, R.G. Roberts and W.J. Stirling, *Phys. Rev.* **D37** (1988) 1161; *Phys. Lett.* **B206** (1988) 327; *Mod. Phys. Lett.* **A4** (1989) 1135.
  22. E. Eichten, I. Hinchliffe, K. Lane and C. Quigg, *Rev. Mod. Phys.*, **56** (1984) 579; *Rev. Mod. Phys.*, **58** (1985) 1065.
  23. J. Morfin and W.K. Tung, *Z. Phys.*, **C52** (1991) 13.
  24. HERWIG 5.8 Program:  
G. Marchesini and B. Webber, *Nucl. Phys.* **B310** (1988) 461;  
I.G. Knowles, *Nucl. Phys.* **B310** (1988) 571;  
G. Marchesini *et al.*, *Comp. Phys. Comm.* **67** (1992) 465.
  25. W.T. Giele, private communication.

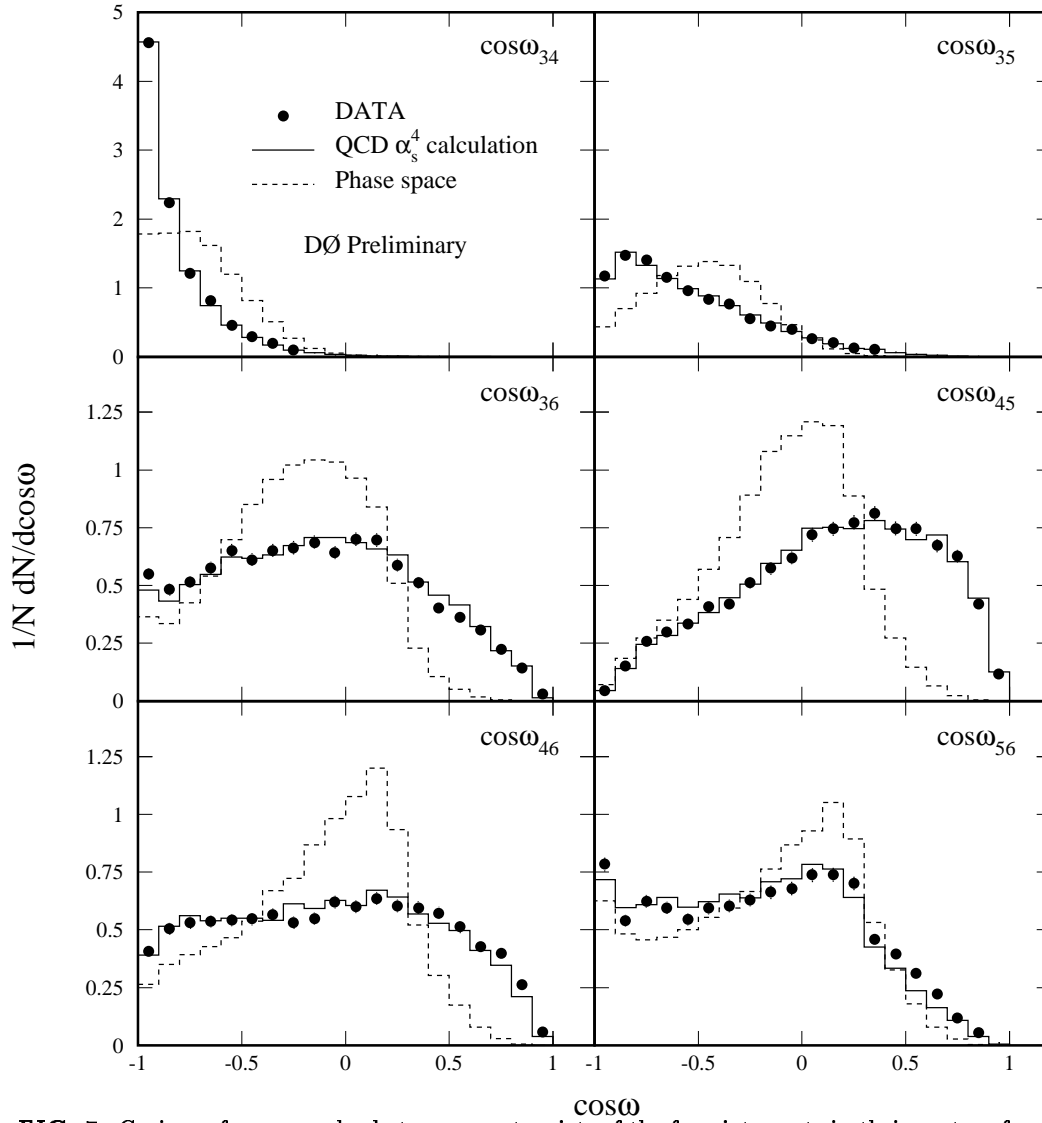


**FIG. 7.** Cosines of space angles between any two jets of the four-jet events in their center-of-mass system. Only statistical errors are shown. The estimated systematic uncertainty on the measurement is 6%.

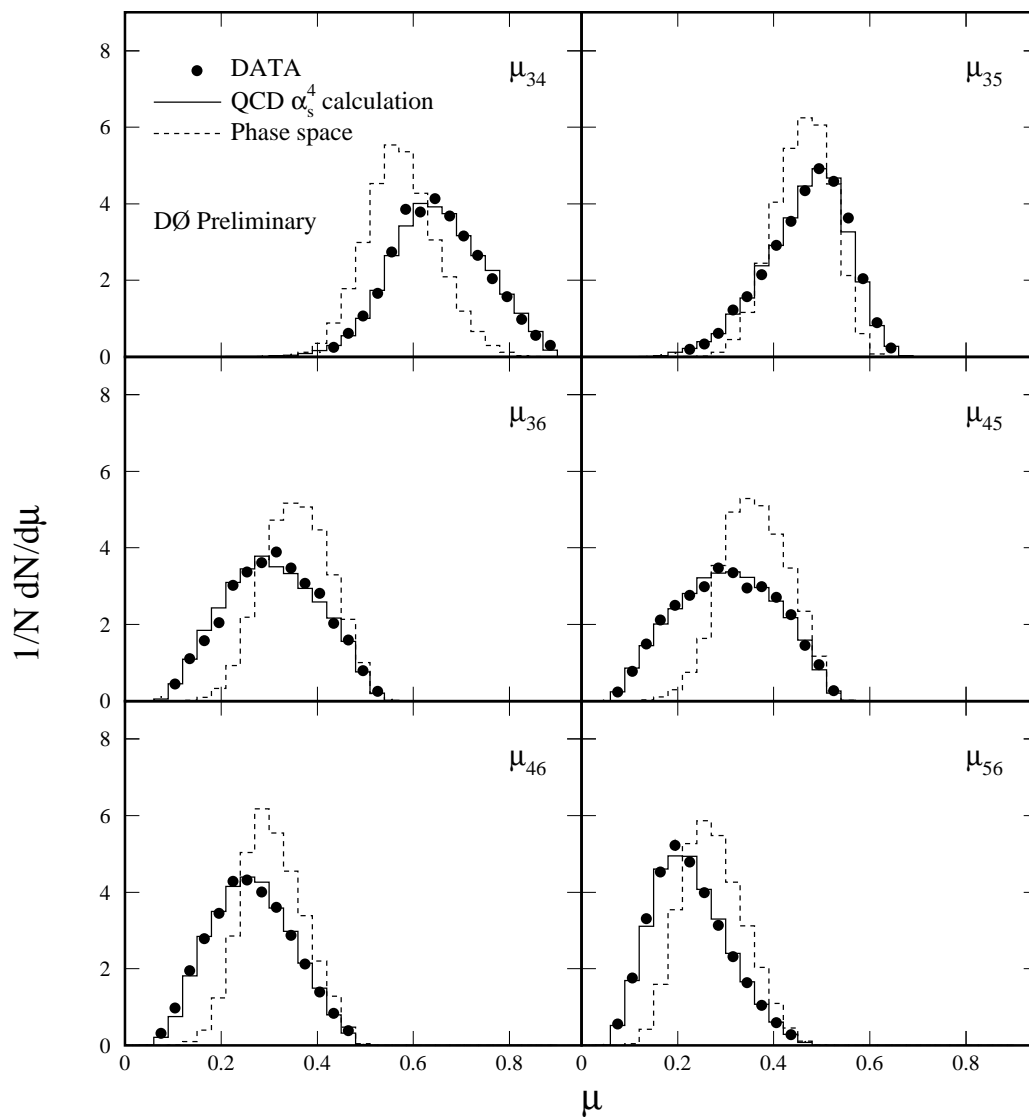


**FIG. 8.** Scaled masses between any two jets of the four-jet events in their center-of-mass system. Only statistical errors are shown. The estimated systematic uncertainty on the measurement is 6%.

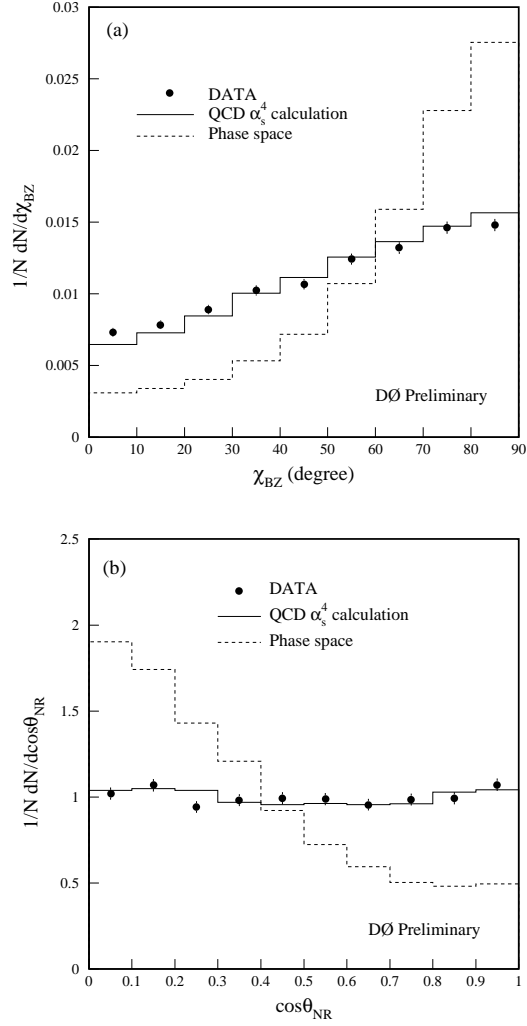


**FIG. 9.** (a) The angle between the plane of the two leading jets and the plane of the two non-leading jets and (b) the angle between the momentum vector differences of the two leading jets and the two non-leading jets of the four-jet events in their center-of-mass system. Only statistical errors are shown. The estimated systematic uncertainty on the measurement is 6%.

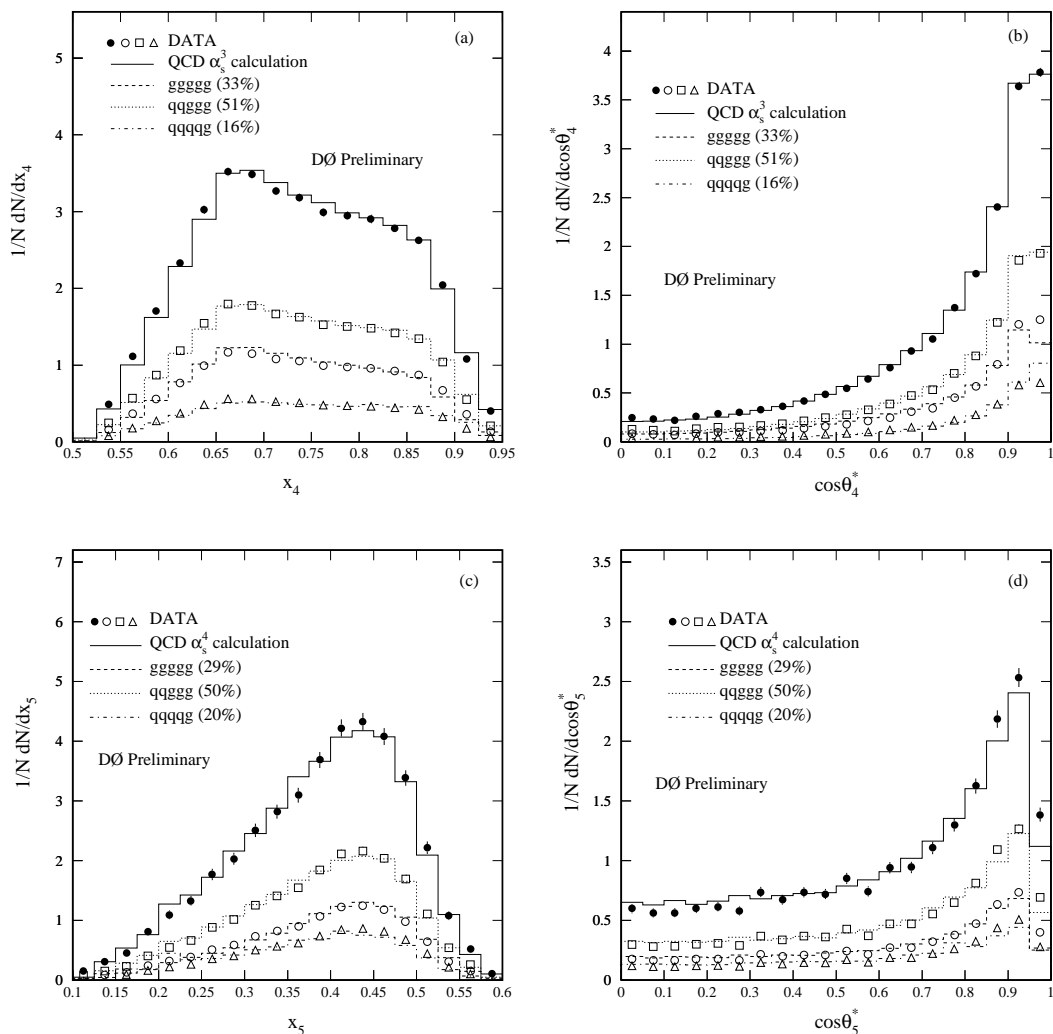


**FIG. 10.** The  $x_4$  (a) and  $\cos\theta_4^*$  (b) distributions of the three-jet events and the  $x_5$  (c) and  $\cos\theta_5^*$  (d) distributions of the four-jet events in their center-of-mass system. The QCD subprocesses are normalized to their fractional contributions to the respective total cross section for the cuts described in the text. The data are normalized to the respective subprocess, therefore, only shapes of the subprocess distributions are compared. Only statistical errors are shown. The estimated uncertainty on the data is less than 6%.